A Novel Approach for Quantifying Magnetic Susceptibility of Aqueous and Organic Solutions

A Novel Approach for Quantifying Magnetic Susceptibility of Aqueous and Organic Solutions

Konrad Wojtaszek[1]*, Andrea Cristofolini[2], Arturo Popoli[2], Karolina K. Siedlecka[1], Marek Wojnicki[1],

[1] - AGH University of Krakow, Faculty of Non–Ferrous Metals, al. A. Mickiewicza 30, 30-059 Krakow, Poland

[2] - Department of Electrical, Electronic and Information Engineering, University of Bologna, 40-136 Bologna, Italy

ABSTRACT: A new method for measuring the magnetic properties of aqueous and organic solutions is presented. This approach is based on quantifying the force resulting from the sample's interaction with a magnetic field. The experimental setup utilizes neodymium magnets attached to a stepper motor to adjust the distance between the magnets and the test sample, while an analytical balance serves as a strain gauge. Magnetic susceptibility measurements were performed on selected inorganic and organic solutions. A series of finite element simulations allowed to convert experimental results to physical quantities describing magnetic susceptibilities of substances. The limit of detection (LoD) and limit of quantification (LoQ) values for the developed method of determining magnetic susceptibility were equal to $6.67 \cdot 10^{-3}$M and $2.02 \cdot 10^{-2}$M, respectively.

1. Introduction.

Magnetic susceptibility is one of the most fundamental physicochemical properties of matter. The magnetic properties of substances can be influenced by several factors, including atomic or molecular structure, electron configuration, and interactions between magnetic moments within the other materials. Different compounds exhibit different magnetic properties, such as paramagnetism, diamagnetism, or ferromagnetism, depending on their magnetic moments and interactions with external magnetic fields [1, 2]. Magnetic susceptibility of varying strength is exhibited by all substances, in every state and form, including the ionic form [2]. The magnetic moment of ions refers to the measure of their magnetic strength or the property that determines their response to an external magnetic field. The magnetic moment is a vector quantity, indicating the direction and magnitude of the magnetic field generated by the ion [1]. The magnetic moment of an ion primarily arises from the presence of unpaired electrons in its electron configuration. Unpaired electrons possess a spin, which generates a magnetic dipole moment. The total magnetic moment of an ion is the vector sum of the magnetic moments of its constituent electrons [3, 4]. The magnetic moment μ of an ion is often expressed in units of Bohr magnetons (μB) [5]. One Bohr magneton is equivalent to the magnetic moment of an electron in its ground state. The magnetic moment of an ion can be calculated based on its electronic structure and the spin and orbital angular momentum of its electrons [6]. For multiple unpaired electrons, the magnetic moment is the vector sum of the individual electron magnetic moments.

It is important to note that the magnetic moment of an ion can vary depending on its electron configuration, oxidation state, and coordination environment [7]. For complex systems, computational determination of the resultant magnetic moment may be difficult, therefore experimental methods of determining magnetic susceptibility are also commonly used.

The magnetic moment of a substance can be measured using various experimental techniques [8]. One of them is Vibrating Sample Magnetometry (VSM) [9]. In this method, the sample is placed in a magnetometer and subjected to an oscillating magnetic field. The resulting induced magnetic moment of the sample is detected and measured, providing information about its magnetic properties. However, VSM is primarily suited for measuring the magnetic properties of ferromagnetic materials [10-15]. Paramagnetic materials, including ions, which have weak magnetic responses, may require specialized techniques or instruments with higher sensitivity to obtain reliable measurements.

Greater sensitivity, allowing to quantitatively measure the magnetic moment of paramagnetic substances, is achieved with the Superconducting Quantum Interference Device (SQUID). The procedure for measuring magnetic properties using the SQUID method involves applying a known magnetic field to a sample, collecting data on its magnetic response, and analysing the data to determine relevant properties such as magnetic moment susceptibility. The measurement is carried out at a temperature close to absolute zero. The measurement time can be up to several days. The sensitivity of the method enables analysis of magnetic fields of 10^{-18} T[16-21].

Another method of determining the magnetic moment is Electron Paramagnetic Resonance (EPR) Spectroscopy which is used to study materials with unpaired electrons, such as paramagnetic ions. By subjecting the ion sample to a magnetic field and varying the frequency of applied microwave radiation, EPR spectroscopy can provide information about the energy levels and transitions associated with the magnetic moment, enabling the determination of its magnitude [22-25]. The Nuclear Magnetic Resonance (NMR) Spectroscopy can also be used to study the magnetic properties. This method is primarily used to study the magnetic properties of atomic nuclei, and can also provide information about the magnetic moments of ions [26-29]. By

analysing the resonance frequencies and relaxation times of the nuclear spins in the presence of a magnetic field, NMR spectroscopy can yield insights into the magnetic properties and moments of the ions [30-33].

In determining the magnetic properties of substances, microscopic methods can also be helpful, such as magnetic force microscopy (MFM) or magneto-optical imaging [34-36]. These techniques allow for the visualization and analysis of the magnetic domains and domain structures within a material [37]. This provides information about the arrangement and behaviour of magnetic moments on a microscopic scale [38-40].

The methods listed above are sophisticated techniques that study magnetic properties at the atomic level. High sensitivity allows us to determine the magnetic moment of the tested particles with very good accuracy. Thus, it allows us to determine the value of the magnetic moment in terms of a physical quantity, limited to narrow, strictly defined conditions of a given research procedure. The data obtained from measurements carried out using the above methods may be of great value for theoretical applications, such as determining specific physical quantities and developing models and mechanisms of phenomena occurring on the atomic scale. However, such data often differ significantly from the resultant value of the magnetic moment that real systems show. High discretization of recorded data for these techniques allows for high accuracy but at the expense of a narrow range of research parameters. Therefore, primary methods are still used in the measurement technique, which can be used to directly test real systems, such as samples with larger masses or volumes compared to the sample size used in NMR or SQUID.

Primary techniques show much lower accuracy, but the experimental data recorded with these methods correspond much better with the magnetic quantity present in the application systems. The methodology is usually based on the measurement of the force generated by the tested sample exposed to the magnetic field [41]. One such technique is Gouy's balance [42-45]. It exploits the principle that the magnetic susceptibility of a material affects its magnetic moment in the presence of an external magnetic field.

Gouy's balance method involves suspending a sample of the material in a non-magnetic holder or tube and subjecting it to a uniform magnetic field. The magnetic field induces a magnetic moment in the sample, which causes it to experience a force within the field. The force acting on the sample is directly proportional to the magnetic field strength, the magnetic susceptibility of the material, and the gradient of the magnetic field. By carefully measuring the displacement of the sample within the magnetic field, Gouy's method allows for the determination of the magnetic susceptibility. Analogous varieties of Gouy's balance are the Faraday balance [46-50] and the Evans balance [51, 52].

It's important to note that Gouy's method assumes that the sample is in the form of a thin rod or wire and that the magnetic field is uniform within the sample volume. Deviations from these assumptions can cause errors in the measurement. This measurement technique is dedicated mainly to solid samples. A variation of Gouy's method adapted to liquid samples, is Quincke's method [53-57]. Quincke's method involves the observation of the behaviour of a liquid within a capillary tube when subjected to an external magnetic field. The setup typically includes a thin glass capillary tube filled with the liquid or solution. The capillary tube is then placed in a uniform magnetic field. When the magnetic field is applied perpendicular to the capillary tube, the liquid level rises, proportional to the applied field and the magnetic moment of the test solution. The difference in liquid levels in the field and without the magnetic field indicates the value of the magnetic susceptibility. However, this method requires a dedicated device, equipped with a strong electromagnet. In addition, its accuracy can be affected by the physicochemical parameters of the liquid being measured, such as density or viscosity. The measurement procedure is adapted to substances having higher magnetic susceptibilities since measuring subtle changes in the height of the liquid column is cumbersome and subject to high error. Therefore, the goal of this research was to develop a method that would not have these limitations.

In the following work, a method of dynamic measurement of the magnetic properties of solutions has been proposed. The data recorded during the experiments provide information on the change in the value of the interaction force between the sample and the field as a function of the shift of the field gradient in the sample volume.

The work analysed the magnetic properties of, among others, holmium solutions. Holmium ion solutions, as an ion with strong paramagnetic properties, as well as organic extractants used for the extraction of rare earth metals, were selected for the study of their magnetic properties. This metal was chosen for experimental work due to one of the highest values of the magnetic moment among the rare earth metals [58, 59]. Rare earth metal ions are characterized by different magnetic properties [60, 61], which can potentially be used in the separation of these metals in hydrometallurgical processes [62-64]. So far, research works on the analysis of the transport of rare earth metal ions under the influence of a heterogeneous magnetic field in both static [59, 65], two-phase [66] and dynamic [67] systems have been developed. Works related to the analysis of the transport of metal ions such as dysprosium, yttrium, europium [68-71] and other rare earth metals ions have appeared in the literature so far. The crucial element in the study of ion migration kinetics is to determine their magnetic susceptibility in the migration medium. The determination of the magnetic susceptibility of rare earth ions in various extraction systems is crucial to the development of research on the use of magnetic fields for obtaining and separating these metals. Measurements of the magnetic properties of other metal ions, i.e. copper and manganese were also performed, as a reference to substances with a correspondingly, high magnetic susceptibility for manganese ions [72, 73] and low magnetic susceptibility for copper ions [74-76]. The Mn(II) ion solution is a standard of the magnetic susceptibility for Quincke's measurement methodology [53]. Experimental measurements were compared with 3D and 2D finite element magnetostatic simulations.

In this work, a new method for determining the magnetic properties of aqueous solutions was proposed. It is assumed that due to the ionic form of holmium, the ions of this metal exhibit different magnetic properties.

1. Experimental.

A test stand for magnetic susceptibility measurements was prepared (**Figure 1**). The measuring element was an analytical balance (Ohaus PA214CM/1, New Jersey, U.S.), marked in **Figure 1** as (1). A spacer made of PVC, marked in **Figure 1** as (2), was placed on the balance pan to eliminate the direct influence of the magnetic field on the balance elements, especially the electronic and weight sensor. Above the analytical balance, on a wooden frame, marked in **Figure 1** as (3), a linear stepper motor, marked in **Figure 1** as (4) was installed. A set of 4 neodymium magnets, marked in **Figure 1** as (5) with a diameter of 20mm,

total height of 40mm and a total magnetic field strength maximum of 0.5387 T was used as the source of the magnetic field. The magnetic field strength of the magnets set was measured using a laboratory Gaussmeter (Lake Shore 475 DSP, Massachusetts, U.S.) The magnets set was attached to the stepper motor, also on the non-magnetic spacer element, to avoid interaction between magnets and the step motor. The analysed sample was placed on the top plane of a spacer placed on the balance pan. A 10mm (optical path length) standard quartz cuvette marked in **Figure 1** as (6) with a volume of 3.7 cm3 (Hellma Analytics) was used as a measuring vessel, covered with a thin microscope slide, with dimensions of 20x20mm and a thickness of 5µm, to reduce evaporation of solutions. In addition, the task of the microscope slide was to obtain a perfectly flat surface of liquid samples analysed in the system. The stepper motor was controlled by a computer application. The choice of the PVC spacer's length was determined based on simulation outcomes. Subsequently, experimental validation was conducted, affirming that the observed alteration in mass is negligible and akin to the balance's inherent drift.

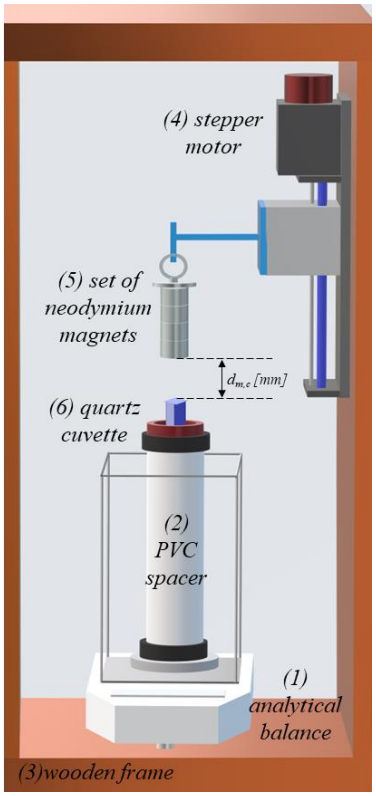

Figure 1 Experimental setup for magnetic susceptibility measurements.

The experiment methodology consisted of gradually approaching a permanent magnet closer to the surface of the solution placed on the balance. The change in the weight recorded on the scales was read and saved by the computer application at a predetermined time interval.

The bottom surface of the magnets in the initial phase of experiments was located at a distance of 30mm from the slide covering the cuvette with the analysed solution. Then, with a step of 5µm microns and a speed of 100 steps per second, the magnets were transported in the direction of the Z axis towards the analysed sample until they reached 5µm the distance from the surface. A certain distance of the magnets from the sample was kept to avoid measurement errors related to the direct contact of the magnets with the sample. The magnets set was kept in this position for 100 seconds and then it was moved away from the sample with the same speed. During this time, the change in the weight of the sample was recorded using an analytical balance with a frequency of 1 second. The transport of the magnets to the sample surface and back was repeated three times in one measurement. The same measurements were repeated at least 3 times.

According to the above procedure, solutions of aqueous holmium ions were measured in concentrations ranging from 0.1 to 1M of holmium ions. The solutions were prepared by dissolving the appropriate amount of holmium (III) chloride (p.a. Onyxmet) in a 0.1M hydrochloric acid solution (p.a. Chempur). In the experimental work, solutions of manganese (II) sulphate (VI) (p.a. Chempur), manganese(II) chloride (p.a. Chempur) and copper(II) sulphate (VI) (p.a. Chempur) in concentrations of 0.1M and 1M were used. The solutions were prepared by dissolving appropriate amounts of salts in 0.1M sulfuric acid (p.a. Chempur) for sulphate solutions and 0.1M hydrochloric acid for chloride solutions. The pH of the solutions was equal to 1 ± 0.05.

Magnetic susceptibility measurements were also carried out for organic compounds such as ethanol (wt. 95% p.a. Chempur), cyclohexane (p.a. Avantor), Verstaic 10 (Hexion), D2EHPA (Baysolvex), and the commercial organic solvent Orlesol 110/170 (Orlen S.A.). To determine the influence of individual elements of the system on the measured values of magnetic susceptibility, the response of the measurement system to the measurement without any sample, with an empty cuvette, and in a cuvette with distilled water (Polwater DL3N-150). was checked. The sample evaporation rate test was carried out to determine the contribution of this phenomenon to the recorded mass change during the actual measurements. The results are presented in this work. The temperature during the measurements was equal to 20 ℃.

The relationship between the magnetic force measured by the analytical balance and the magnetic susceptibility of the solution in the cuvette was evaluated numerically. Using the COMSOL Multiphysics 6.1 software (AD/DC module), the magnetostatic problem consisting of:

$$\nabla \times H = J$$
$$\nabla \times B = 0$$

and the material constitutive relation expressing the magnetic flux density $\boldsymbol{B}$ as a function of the magnetic field $\boldsymbol{H}$:

$$B = B(H)$$

was solved through a finite element analysis. Particularly, the aqueous solution was assumed to behave as homogeneous, isotropic, and linear material and is thus described by the constitutive relation:

$$B = \mu_{sol} H$$

where the aqueous solution magnetic permeability μ_{sol} can be expressed as a function of the solution dimensionless magnetic susceptibility χ_{sol}:

$$\mu_{sol} = \mu_0 (1 + \chi_{sol})$$

The magnetic susceptibility χ_{sol} depends on the composition of the considered solution. In an aqueous solution with n chemical species with molar concentration and molar susceptibility c_k and χ_k, respectively, the solution susceptibility χ_{sol} can be expressed as:

$$\chi_{sol} = \chi_{H_2O} + \sum_{k=1}^{n} c_k \chi_k$$

where χ_{H_2O} is the dimensionless magnetic susceptibility of water. According to the above-mentioned homogeneity assumption, χ_{sol} is considered uniform over the entire solution. The magnetic force acting on the cuvette has been obtained by integrating the Maxwell stress tensor $\overleftrightarrow{\boldsymbol{T}}$ on a closed surface encompassing the cuvette. In the framework of the magnetostatic formulation, the Maxwell stress tensor takes the form:

$$\overleftrightarrow{T} = \frac{1}{\mu_0}(BB - \frac{1}{2}B^2\overleftrightarrow{I})$$

where $\overleftrightarrow{\boldsymbol{I}}$ is the identity tensor.

2. Measurements of magnetic properties.

3.1 Metals ions solutions.

Using the prepared experimental system (**Figure 1**), measurements of the magnetic properties of selected substances were carried out. The value read directly from the analytical balance during the measurement was the weight of the sample. Typically, the weight of a sample depends on its mass, the other components being relatively constant. As it is known, the mass of the sample did not change during the measurement. Its weight changed because the resultant of the forces making up the value of the sample weight was accompanied by a third component, which was the value of the force of attraction or repulsion of the sample towards the magnet, directly proportional to the value of the magnetic susceptibility of the tested sample. For simplicity, the term "apparent mass change" is used in the analysis of the results.

The results for the measurement of the solution of Ho(III) with a concentration of 1M are shown in **Figure 2**. The OY axis shows the apparent change in the mass of the sample during the measurement.

Figure 2 A) presents the apparent mass change recorded on the analytical balance during a single experiment cycle consisting of moving the magnets from zero point (I) to the sample surface (II-III), holding the magnets in this position for 100 sec (III) and moving them away from the surface (IV-V), back to the zero point (VI). Knowing the speed of the magnet's movement and the exact distances of the sample from the magnets during the measurement cycle, the measurement results were presented as a function of the distance of the magnet relative to the sample surface. **Figure 2** B) thus shows the mass change recorded on the balance depending on the distance of the magnet from the sample. The formation of a hysteresis loop was observed; therefore it can be assumed that some ions shifting in the solution occurred under the influence of the approaching magnetic field.

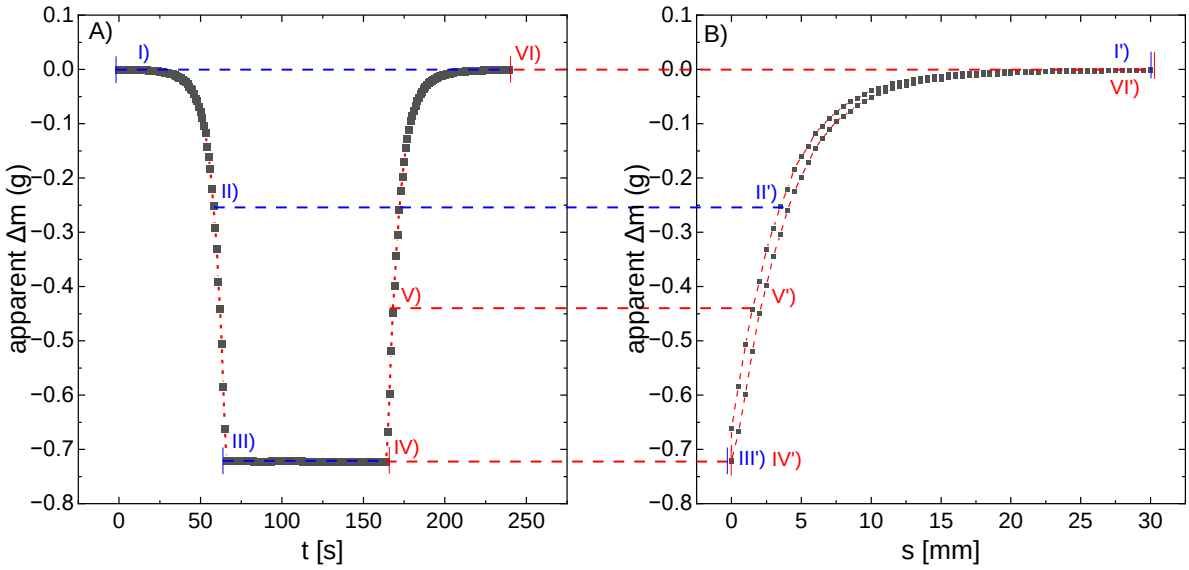

Figure 2 Apparent mass changes of the sample of a 1M solution of Ho(III) ions as a function of A) measurement time, and B) distance of the magnet from the sample surface.

Similarly to the 1M concentration shown in **Figure 2**, measurements were carried out for other concentrations of Ho(III) ions. The results are summarized in **Figure 3** The values read for the 120th second of the measurement, as representative, were averaged for at least 3 independent measurements of the same sample. The relative standard deviation of the results for all concentrations was within Relative Standard Deviation RSD<1.1%. The zero concentration value was the measurement for a sample of demineralized water, for which, after 5 repetitions, the average of results with the value of RSD=2.12% was obtained. A linear relation of this function was determined with the coefficient R^2 equal to 0.999. The standard deviation for each measurement point is shown in the graph as error bars. The value of this parameter has been multiplied by 10, otherwise, the error bars would not be visible on the chart.

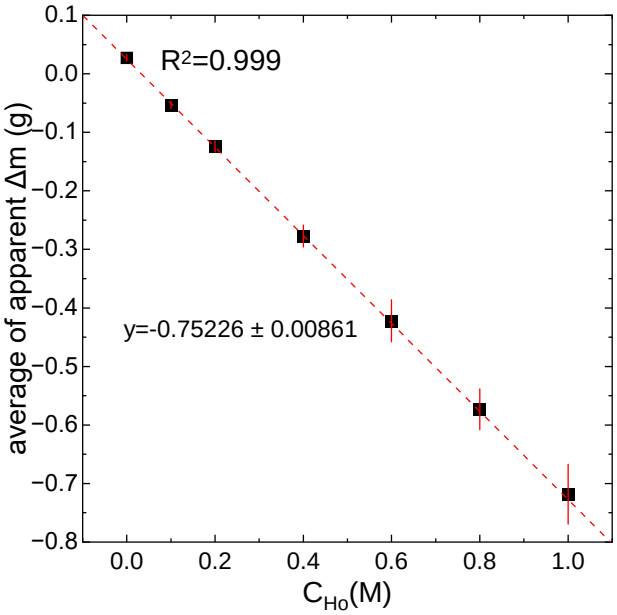

Figure 3 The influence of Ho(III) initial concentration on the apparent mass changes.

Measurements were also carried out for manganese (II) ions, as a standard of magnetic susceptibility found in the literature [72, 73]. The course of a single experiment with a 1M solution of Mn(II) ions in chloride solution (see **Figure 4**) was analogous to the measurement of a 1M solution of Ho(III) ions. In this case, however, the recorded values were much lower, which proves that the magnetic susceptibility of Mn(II) ions is lower than that of Ho(III).

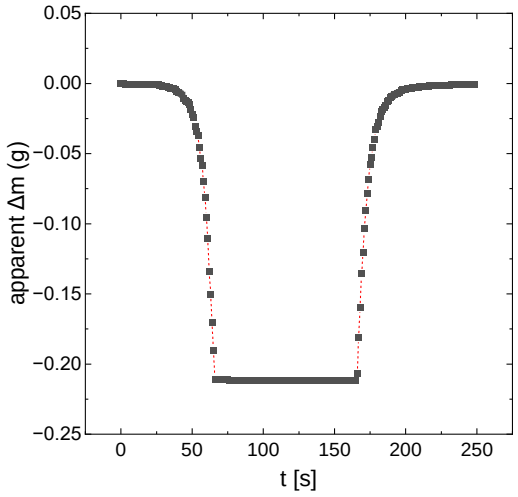

Figure 4 Apparent mass changes of the sample of a 1M solution of Mn(II) (Cl-) ions as a function of A) measurement time, and B) distance of the magnet from the sample surface.

The results for solutions of manganese (II) chloride with a concentration of 1M, 0.1M and water as a zero concentration are presented in **Figure 5**. This graph has also a linear relation and contains information about the standard deviation for each measurement point, and this value is also multiplied by 10 for better clarity of the figure.

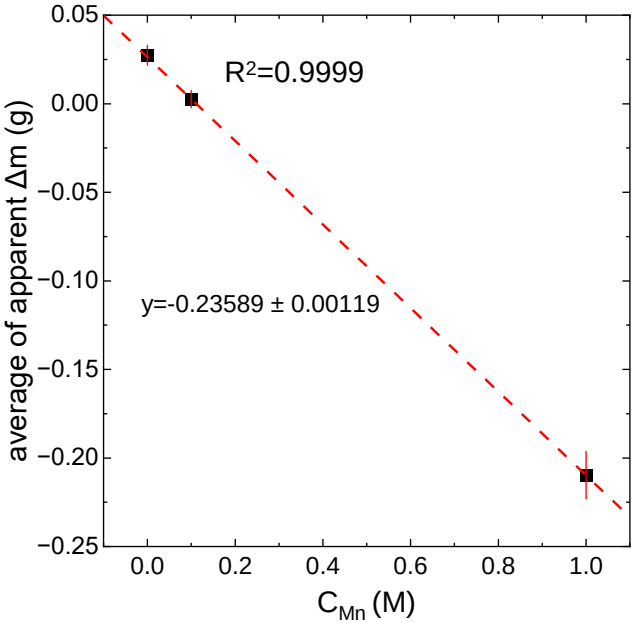

Figure 5 The influence of Mn(II) (Cl-) initial concentration on the apparent mass changes.

The exact values and other results for the measurements of Mn(II) ions in the sulphate and chloride medium, and Cu(II) ions in the sulphate medium are presented in **Table 1**.
As can be seen, the magnetic susceptibility of Cu(II) ions is much lower than the magnetic susceptibility of Mn(II) ions.

On the other hand, a significant difference in the results for Mn(II) ions in the sulphated and chloride medium proves that the metal ion environment affects its magnetic susceptibility.

Table 1 Results of magnetic susceptibility measurements for Cu(II) and Mn(II) ions.

Substance	Apparent Δm [g]	*σ [%]*
0 (H_2O)	0.02734	2.12
$CuSO_4$ 0.1M (aq)	0.02816	0.54
$CuSO_4$ 1M (aq)	0.00195	0.08
$MnSO_4$ 0.1M (aq)	0.6566	4.68
$MnSO_4$ 1M (aq)	-0.3077	0.22
$MnCl_2$ 0.1M (aq)	0.002633333	0.05
$MnCl_2$ 1M (aq)	-0.20973333	0.13

3.2 Organic and inorganic solvents

The values of mass change and RSD for inorganic acids solutions and organic solvents were measured analogously, the results are presented in **Table 2**. In the case of inorganic substances, the mass change is small, reaching a maximum of approx—0.027 g. The relative standard deviation in the case of sulfuric acid is equal to 0.05%, which proves a very good repeatability of measurements and stability of this solution. On the other hand, in the case of organic substances, both greater

weight changes and higher RSD values are observed. This is probably because the molecules of organic substances are larger, and therefore their diffusion is difficult. Another reason for this may be intermolecular interactions.

Table 2 Results of magnetic susceptibility measurements for organic and inorganic substances.

Substance	Δm [g]	*σ[%]*
H_2O	0.02734	2.12
0.1M H_2SO_4 aq	0.02773	0.05
0.1M HCl aq	-0.01755	1.13
Ethanol wt.95% aq	-0.30416	1.55
Orlesol 110/170	-1.0087	11.71
cyclohexane	-0.96935	14.87
D2EHPA	0.0241	0.17
Verstatic 10	-0.2094	3.43

The elevated magnetic susceptibility of organic compounds is elucidated in the study conducted by Jeremy I. Musher [77]. This investigation reveals that the non-uniform magnetic characteristics detected in aromatic hydrocarbons, often ascribed to the π-electron "ring currents," can be accurately comprehended as a composite outcome stemming from contributions of localized electrons of both π and σ natures. The supposition of electronic distribution being "delocalized" does not exert a substantive influence; rather, it emerges primarily as a consequence of London's approximative computation. The empirical approach was employed to ascertain specific values, referred to as Pascal's constants, pertinent to aromatic carbon atoms. Intriguingly, these constants exhibit a remarkable alignment with the magnetic properties observed within experimental settings.

3. Numerical simulations

FEM analysis was used to calculate the magnetic field produced by the permanent magnets at various positions of the cuvette. The analysis was conducted using both two-dimensional and three-dimensional geometric models.

For a 2D case, the computational problem could be solved using a magnetic vector potential formulation as in [78, 79]. However, thanks to the absence of free currents, one has $J = 0$ in Eq. $\nabla \times H = J$, which yields a magnetic field that is irrotational in every point of the considered geometry. In this case, one may define a scalar potential ψ such that $\boldsymbol{H} = -\nabla\psi$, which allows to operate with a scalar Poisson-type problem in both the 2D and 3D cases. The specific geometry of the considered problem would require a three-dimensional model, due to the non-cylindrical shape of the cuvette.

However, for a given mesh size, a 3D FEM model involves a much greater computational load than a 2D one. In this respect, the force calculation through the described surface integration of Maxwell's stress tensor presents some criticalities, since it requires great accuracy and, therefore, a very refined calculation mesh. While introducing an approximation in the geometric shape of the cuvette, a 2D FEM analysis allows to obtain adequate mesh refinements more easily. For the 2D calculations discussed in this work, an axisymmetric r-z geometry was used, i.e., the solution in the cuvette was represented as a cylinder. Its radius $r_{c,2D}$ has been selected so that the real cuvette and the cylindrical one in the 2D approximation have equal volumes:

$$r_{c,2D} = \sqrt{\frac{w_c \cdot d_c}{\pi}}$$

where w_c and d_c are the real cuvette width and depth, respectively.

Figure 6 shows two plots representing the magnetic flux density distributions as computed by the 2D and 3D models. The 3D result in **Figure 6** B) also shows part of the employed mesh. A structured hexahedral mesh has been used for the cuvette and the air gap between the cuvette and the magnet. The cylindrical magnet has been subdivided into an inner (square section) and an out region. The square section inner region has been discretized once again with a structured hexahedral mesh, contiguous to the one used for the air gap, while the outer region has been obtained by extruding a superficial layer of unstructured triangles. The thickness of the hexahedral elements in the air gap decreases from the magnet surface to the cuvette surface. This feature is necessary for two reasons: first, to limit the overall amount of mesh elements when large values of $d_{m,c}$ are employed, and secondly to create a boundary layer-like structure with respect to the cuvette region, which considerably increases the accuracy of the Maxwell stress tensor integration. The magnetic flux density trend along the axis of the cuvette is shown in **Figure 7**. Here, the magnet surface closer to the cuvette is taken as a reference for the axial distance reported on the abscissae axis. The calculation mesh used for the 3D models requires about $8 \cdot 10^5$ tetrahedral elements, with a minimum characteristic dimension of a few tenths of a millimeter. Conversely, meshes constituted by $\sim 8 \cdot 10^4$ triangles have been used for 2D calculations, with minimum characteristic sizes similar to the ones reported for the 3D case.

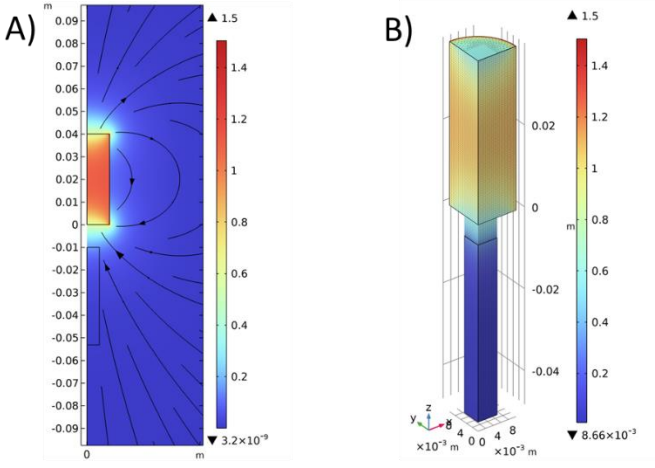

Figure 6 Magnetic flux density in the magnet (top) and cuvette (bottom) from 2D (A) and 3D (B) calculations when d(m,c)=1 mm. In the 3D case, only one quarter of the physical domain has been considered, thanks to the symmetry of the problem

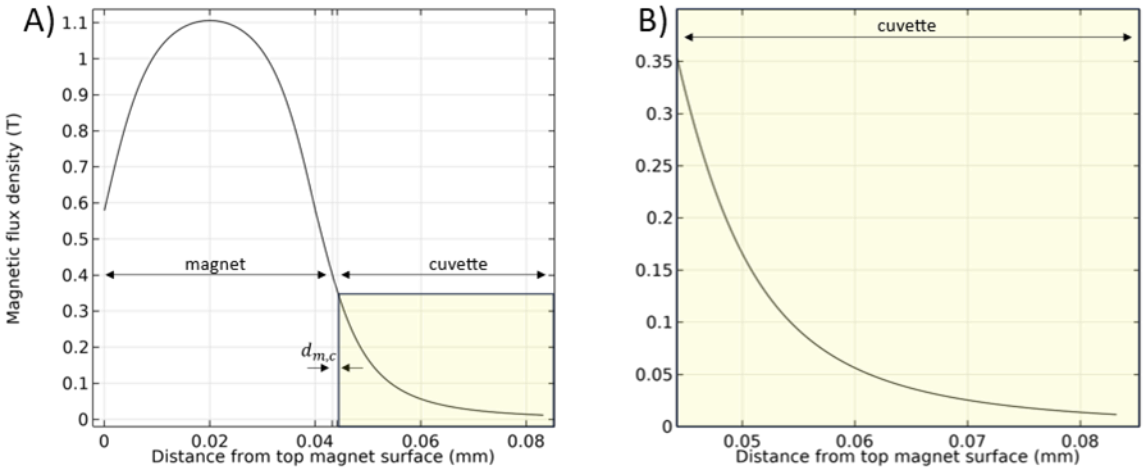

Figure 7 A) Magnetic flux density on the axis of the magnet-cuvette system, computed via the 3D FEM approach when the distance $d_{(m,c)}$ between the facing surfaces of the cuvette and the magnet is 0.5 mm. B) Detail of the computed magnetic flux density along the cuvette axis.

4.1 Experimental magnetic susceptibility determination.

The magnetic susceptibility of the aqueous solution has been iteratively adjusted so that the numerically calculated force fits the experimental result. In **Figure 8** the obtained fits were obtained with the 2D and 3D models at different Ho(III) concentrations. It is worth noting that for each concentration, a single magnetic susceptibility value was identified, which was used for both 2D and 3D calculations. The magnetic susceptibility value is reported in the top-right corner of each subfigure in **Figure 8**.

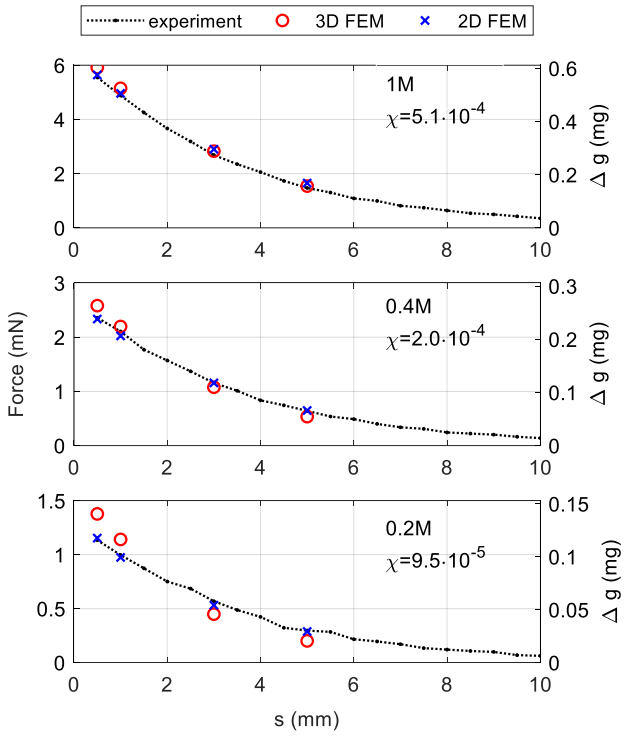

Figure 8 Comparison of the measured magnetic force acting on the cuvette at various distances from the magnets with the 2D and 3D computations at different holmium concentrations.

The computations show a good agreement between the results of the 2D and 3D approaches. Thus, exploiting the lower computational burden and the absence of critical issues of the 2D model, a force map was obtained as a function of the dimensionless magnetic susceptibility and the distance of the cuvette from the magnets. This map, shown in **Figure 9**, can be used to estimate the magnetic susceptibility of any solution within the considered range for χ.

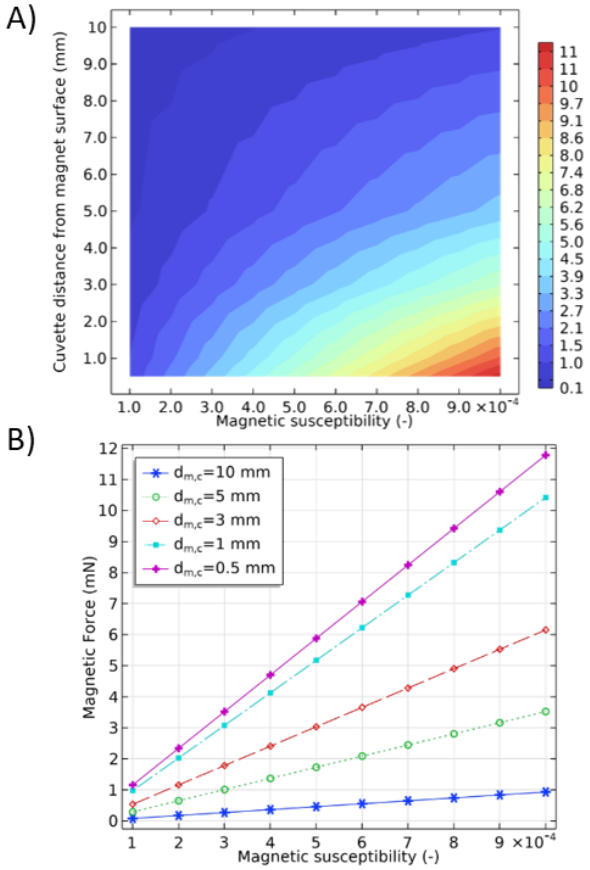

Figure 9 Magnetic force (mN) for different values of magnetic susceptibility and cuvette distance from the magnet surface, obtained via a series of parametric 2D FEM simulations. The force values are presented as a 2D map (A) and as a series of line plots (B).

The Ho(III) molar susceptibility χ_{Ho} has been evaluated through equation, neglecting the contribution of chlorine ions to the solution susceptibility:

$$\chi_{Ho} = \frac{\chi_{sol} - \chi_{H_2O}}{C_{Ho}}$$

A dimensionless magnetic susceptibility of $\chi_{H_2O} = -9 \cdot 10^{-6}$ has been taken for water [80]. The Ho(III) molar susceptibility resulting from the solution susceptibility values obtained for the three cases shown in **Figure 8** are reported in **Table 3**.

Table 3 Ho(III) molar susceptibility resulting from three different concentrations.

C[mol/l]	χ_{sol}	χ_{Ho}[m^3/mol]
1.0	$5.1 \cdot 10^{-4}$	$5.19 \cdot 10^{-7}$
0.4	$2.0 \cdot 10^{-4}$	$5.23 \cdot 10^{-7}$
0.2	$9.5 \cdot 10^{-5}$	$5.20 \cdot 10^{-7}$

5. Experimental error analysis

To quantify the influence of external factors on the test results, a series of measurements was carried out for systems without test samples. The course of these baseline experiments was analogous to the actual measurements for the test samples. The measurement consisted of moving the magnet by a given distance, stopping for a certain time and then returning the magnet to its starting position. During this time, the weight change was recorded.

First, a measurement without a sample was performed to investigate the balance drift in a time corresponding to that of a standard experiment. Three replicates of the experiment were performed. The average weight change resulting from balance drift was $1.57 \cdot 10^{-4}$ g with a RSD<0.01%.

Then, the magnetic properties of an empty quartz cuvette with a microscope slide were measured. The mean value of change in weight recorded for three replicates of the experiment was $-5.28 \cdot 10^{-3}$g with an RSD<0.2%.

The evaporation rate of 0.1 M hydrochloric acid solution as the base solution for the tested samples was also tested. In this case, the measurement was static and consisted of leaving the cuvette with the solution for a certain time and recording the mass change during this time. A coverslip was used during the measurements, analogous to the course of standard experiments. The measurement was made in the presence of a magnetic field when the magnet was placed directly at the surface of the sample and in the version without the magnet. The measurement results are shown in **Figure 10**.

This experiment was carried out to determine how the mass loss of the sample due to evaporation will affect the result of the magnetic susceptibility measurement. As can be seen in **Figure 10**, the mass loss caused by evaporation during the measurement has a negligible effect on the total measurement result.

Interestingly, it was noticed that the waveform of the evaporation curve for the sample exposed to the magnetic field is different from the sample without the magnetic field. This suggests that the presence of an external magnetic field may affect the rate of solution evaporation. The proposed method is perfectly suited to study this type of effect.

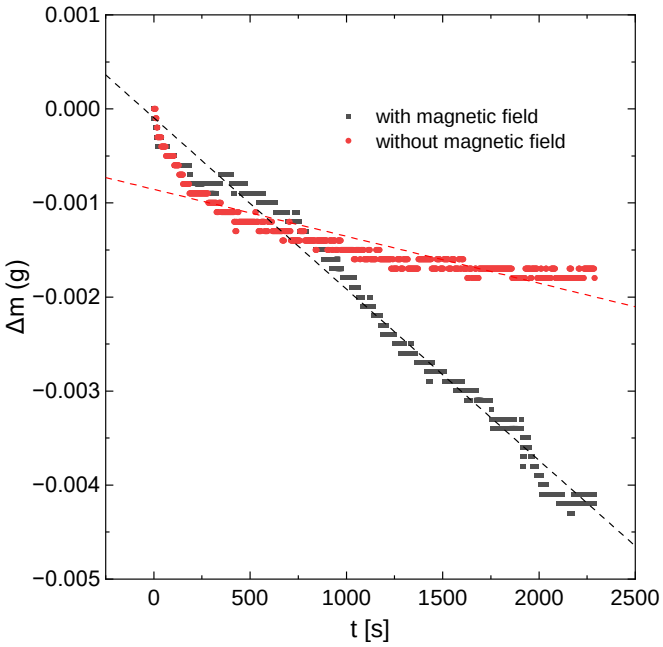

Figure 10 Mass changes during evaporation of a 0.1 M HCl solution, in the presence of a magnetic field and without a magnetic field.

Measurement stability and analytical balance drift tests were carried out. For this purpose, the measurement was run without any sample for 6 hours with a mass reading every 15 minutes. The recorded weight drift was below +/- $1 \cdot 10^{-4}$ g/h.

The accuracy and repeatability of the measurements strictly depended on the precision of the stepper motor used, so the test was carried out using a dial indicator with a pitch of 10/0.01mm (Limit 10/0.01, Alingsås, Sweden). The test consisted of installing a dial indicator on a tripod in the place where the sample was located during the standard experiment, setting the zero point. Then, the course of the stepper motor was set for the maximum distance and then returned to the zero point. The experiment was repeated 8 times, each time recording the indications of the dial gauge. The results indicate that the average divergence from the zero point is -2.37μm, with a standard deviation of 3.48μm. The drift of subsequent measurements did not have a linear relationship, which means that the stepper motor has its error, but it does not "lose steps".

6. LoD, LoQ calculation

Based on the results of measurements of the magnetic susceptibility of solutions of Ho(III) ions of various concentrations (see **Figure 3**), the LoD (limit of detection) and LoQ (limit of quantification) of the developed analytical method were calculated. The detection limit is the lowest concentration or amount of a substance that can be reliably detected, but not necessarily quantified, with a given analytical method. It represents the point at which the signal generated by the substance is distinguishable from background noise, usually expressed as a signal-to-noise ratio.

The quantification limit is the lowest concentration or amount of a substance that can be accurately measured and quantified with a given analytical method. It is a more stringent criterion than the detection limit, as it ensures that the

measurement results fall within an acceptable range of accuracy and precision.

For the developed graph (**Figure 3**), the value of the σ is equal to 0.00152, while the value of the S is equal to -0.75226. The value of the S parameter for the calculations was assumed in the absolute value.

Accordingly, the calculated LoD value is $6.67 \cdot 10^{-3}$ while the LoQ is $2.02 \cdot 10^{-2}$.

Since the value of S refers to the OX axis in the graph, LoD and LoQ refer to the same unit, i.e. the concentration in $\frac{\mathrm{mol}}{\mathrm{dm}^3}$.

7. Conclusions:

The presented methodology for determining the magnetic susceptibility of materials is characterized by significant sensitivity, enabling the measurement of organic and inorganic substances. Using the proposed measurement setup, measurements of the magnetic susceptibility of solutions of selected metal ions, inorganic acids and selected organic solutions were carried out. As a methodological example, measurement results for holmium(III) ions solutions were developed using numerical simulations, which allowed for the extraction of magnetic susceptibility values. The obtained molar magnetic susceptibility of holmium (III) ions in a solution with a concentration of 1M was $5.19 \cdot 10^{-7}\ \mathrm{m}^3/\mathrm{mol}$, with an external field intensity acting on the sample of 0.5387 T. This indicates a high magnetic susceptibility of holmium(III) ions, which is in good agreement to the literature [81-83].

Comparing the results obtained directly from measurements on an analytical balance, it can be concluded that a solution of manganese(II) ions at a concentration of 1M has a magnetic susceptibility value that is more than three times lower than a solution of holmium(III) ions. It is also significant that the anion conjugated to the tested cation is also important. Manganese (II) ions in a chloride environment show much lower magnetic susceptibility than in a sulphate (VI) ion environment. Copper ions, similarly to metal in bulk form, have a much lower magnetic susceptibility than holmium or manganese.

Surprisingly high values were recorded for selected organic substances. Ethanol with a concentration by weight of 95% showed a magnetic susceptibility almost equal to a 1M solution of manganese(II) sulfate. However, cyclohexane and the commercial organic solvent Orlesol 110/110 showed a magnetic susceptibility more than three times higher than that of ethanol, reaching the highest recorded value. The organic compound D2EHPA showed a marginally low magnetic susceptibility, while Versatic 10 showed a high magnetic susceptibility, equaling the susceptibility value recorded for a 1M manganese(II) chloride solution. We suggest, that the difference in magnetic properties of some organic compounds can be used for their detection/determination and separation in HPLC (High-Pressure Liquid Chromatograph) and/or UHPLC (Ultra High-Pressure Liquid Chromatograph).

The large differences in the recorded results result from a large number of parameters that can affect the magnetic properties of the solutions, especially under the influence of an external magnetic field [84]. This opens new horizons for research on the physicochemical properties of substances and reactions in a magnetic field. This predicts a wide application of methods that allow for the study of the magnetic properties of solutions. The presented methodology allows for quantitative quantification of the magnetic susceptibility of almost any substance, using a relatively simple experimental system. Moreover, the very analysis of direct results, expressed in the form of an apparent change in mass, provides preliminary information about the magnetic properties of the tested substance during the measurements. This allows us to determine optimal measurement conditions without the need to perform numerical analyses each time.

The above work presents the concept of the measurement method, along with examples of application. Optimization of both the experimental and numerical parts can further increase the sensitivity and accuracy of the measurement method. Additional work within this area is scheduled for the future.

AUTHOR INFORMATION

Corresponding Author

*E-mail: kwojtasz@agh.edu.pl, Phone: +48664993026

Author Contributions

All authors contributed to writing the manuscript and have approved the final version.

Notes

The authors declare no competing financial interest.

REFERENCES

(1) Zatsiupa, A. A.; Bashkirov, L. A.; Troyanchuk, I. O.; Petrov, G. S.; Galyas, A. I.; Lobanovsky, L. S.; Truhanov, S. V. Magnetization, magnetic susceptibility, effective magnetic moment of Fe3+ ions in Bi25FeO39 ferrite. Journal of Solid State Chemistry 2014, 212, 147-150. DOI: https://doi.org/10.1016/j.jssc.2014.01.019.

(2) Yung, K. W.; Landecker, P. B.; Villani, D. D. An Analytic Solution for the Force Between Two Magnetic Dipoles. Magnetic and Electrical Separation 1998, 9, 079537. DOI: 10.1155/1998/79537.

(3) Cullity, B. D.; Graham, C. D. Introduction to Magnetic Materials; Wiley, 2009.

(4) Krey, U.; Owen, A. Basic Theoretical Physics, A Concise Overview. Basic Theoretical Physics: A Concise Overview 2007. DOI: 10.1007/978-3-540-36805-2.

(5) Mugiraneza, S.; Hallas, A. M. Tutorial: a beginner's guide to interpreting magnetic susceptibility data with the Curie-Weiss law. Communications Physics 2022, 5 (1), 95. DOI: 10.1038/s42005-022-00853-y.

(6) Prigogine, I.; Rice, S. A. Advances in chemical physics. Vol. 116; Wiley New York, 2001.

(7) Boyer, T. H. The force on a magnetic dipole. American Journal of Physics 1988, 56 (8), 688-692. DOI: 10.1119/1.15501 (acccessed 10/8/2023).

(8) Foner, S. Review of magnetometry. IEEE Transactions on Magnetics 1981, 17 (6), 3358-3363. DOI: 10.1109/TMAG.1981.1061748.

(9) Dodrill, B.; Lindemuth, J. R. Vibrating Sample Magnetometry. In Magnetic Measurement Techniques for Materials Characterization, Franco, V., Dodrill, B. Eds.; Springer International Publishing, 2021; pp 15-37.

(10) Singha, K.; Jasrotia, R.; Singh, V. P.; Chandel, M.; Kumar, R.; Kalia, S. A study of magnetic properties of Y–Ni–Mn substituted Co2Z-type nanohexaferrites via vibrating sample magnetometry. Journal of Sol-Gel Science and Technology 2021, 97 (2), 373-381. DOI: 10.1007/s10971-020-05412-x.

(11) Frandsen, B. A.; Read, C.; Stevens, J.; Walker, C.; Christiansen, M.; Harrison, R. G.; Chesnel, K. Superparamagnetic dynamics and blocking transition in ${\mathrm{Fe}}_{3}{\mathrm{O}}_{4}$ nanoparticles probed by vibrating sample magnetometry and muon spin relaxation. Physical Review Materials 2021, 5 (5), 054411. DOI: 10.1103/PhysRevMaterials.5.054411.

(12) Hioki, T.; Ohkubo, M.; Itoh, A.; Doi, H.; Kawamoto, J.-i.; Kamigaito, O. Vibrating Sample Magnetometry of High-Tc Superconductor Y-Ba-Cu Oxide. Japanese Journal of Applied Physics 1987, 26 (5A), L636. DOI: 10.1143/JJAP.26.L636.

(13) Ohodnicki, P. R.; Goh, K. Y.; McHenry, M. E.; Ziemer, K.; Chen, Z.; Vittoria, C.; Harris, V. G. Correlation between texture, anisotropy, and vector magnetization processes investigated by two-dimensional vector vibrating sample magnetometry in BaO(Fe2O3)6 thin film. Journal of Applied Physics 2008, 103 (7). DOI: 10.1063/1.2838630 (acccessed 10/8/2023).
(14) Camelo, K. J.; Oliveira Junior, F. C.; da Silva, M. R.; Vasconcelos, I. F. Influence of precipitates on the magnetic properties of Fe–Cr–Mo alloys studied by X-ray diffraction, Mössbauer spectroscopy and vibrating sample magnetometry. Journal of Materials Research 2017, 32 (7), 1316-1323. DOI: 10.1557/jmr.2016.525 From Cambridge University Press Cambridge Core.
(15) Nishio, H.; Machida, K. I.; Ozaki, K. More Accurate Hysteresis Curve for Large Nd–Fe–B Sintered Magnets Employing a Superconducting Magnet-Based Vibrating Sample Magnetometer. IEEE Transactions on Magnetics 2017, 53 (4), 1-6. DOI: 10.1109/TMAG.2016.2641399.
(16) Pandhare, A. B.; Patil, R. P.; Delekar, S. D. 19 - Metal oxide-based composites for magnetic hyperthermia applications. In Advances in Metal Oxides and Their Composites for Emerging Applications, Delekar, S. D. Ed.; Elsevier, 2022; pp 673-695.
(17) Fagaly, R. L. Superconducting quantum interference device instruments and applications. Review of Scientific Instruments 2006, 77 (10). DOI: 10.1063/1.2354545 (acccessed 10/8/2023).
(18) Kleiner, R.; Koelle, D.; Ludwig, F.; Clarke, J. Superconducting quantum interference devices: State of the art and applications. Proceedings of the IEEE 2004, 92 (10), 1534-1548. DOI: 10.1109/JPROC.2004.833655.
(19) Koelle, D.; Kleiner, R.; Ludwig, F.; Dantsker, E.; Clarke, J. High-transition-temperature superconducting quantum interference devices. Reviews of Modern Physics 1999, 71 (3), 631-686. DOI: 10.1103/RevModPhys.71.631.
(20) Hasselbach, K.; Mailly, D.; Kirtley, J. R. Micro-superconducting quantum interference device characteristics. Journal of Applied Physics 2002, 91 (7), 4432-4437. DOI: 10.1063/1.1448864 (acccessed 10/8/2023).
(21) Greenberg, Y. S. Application of superconducting quantum interference devices to nuclear magnetic resonance. Reviews of Modern Physics 1998, 70 (1), 175-222. DOI: 10.1103/RevModPhys.70.175.
(22) Che, M.; Giamello, E. Chapter 5 Electron Paramagnetic Resonance. In Studies in Surface Science and Catalysis, Fierro, J. L. G. Ed.; Vol. 57; Elsevier, 1990; pp B265-B332.
(23) Baumann, S.; Paul, W.; Choi, T.; Lutz, C. P.; Ardavan, A.; Heinrich, A. J. Electron paramagnetic resonance of individual atoms on a surface. Science 2015, 350 (6259), 417-420. DOI: doi:10.1126/science.aac8703.
(24) Abragam, A.; Bleaney, B. Electron paramagnetic resonance of transition ions; Clarendon P. Oxford, 1970.
(25) Weil, J. A.; Bolton, J. R. Electron Paramagnetic Resonance: Elementary Theory and Practical Applications; Wiley, 2007.
(26) Sugimoto, K.; Mizobuchi, A.; Nakai, K.; Matuda, K. Magnetic Moment of F17 – Nuclear Magnetic Resonance by Polarization Following O16 (d, n) F17 Reaction –. Journal of the Physical Society of Japan 1966, 21 (2), 213-221. DOI: 10.1143/JPSJ.21.213 (acccessed 2023/10/08).
(27) Antušek, A.; Repisky, M.; Jaszuński, M.; Jackowski, K.; Makulski, W.; Misiak, M. Nuclear magnetic dipole moment of $^{209}\mathrm{Bi}$ from NMR experiments. Physical Review A 2018, 98 (5), 052509. DOI: 10.1103/PhysRevA.98.052509.
(28) Makulski, W.; Słowiński, M. A.; Garbacz, P. Nuclear Dipole Moments and Shielding Constants of Light Nuclei Measured in Magnetic Fields. Magnetochemistry 2023, 9 (6), 148.
(29) Hughes, J. G.; Lawson, P. J. An application of the NMR method for determination of magnetic moments to study anomalous paramagnetism in some iron(III) chelates. Journal of Chemical Education 1987, 64 (11), 973. DOI: 10.1021/ed064p973.
(30) Bovey, F. A.; Mirau, P. A.; Gutowsky, H. S. Nuclear Magnetic Resonance Spectroscopy; Elsevier Science, 1988.
(31) Darbeau, R. W. Nuclear Magnetic Resonance (NMR) Spectroscopy: A Review and a Look at Its Use as a Probative Tool in Deamination Chemistry. Applied Spectroscopy Reviews 2006, 41 (4), 401-425. DOI: 10.1080/05704920600726175.
(32) Lee, S.; Richter, W.; Vathyam, S.; Warren, W. S. Quantum treatment of the effects of dipole–dipole interactions in liquid nuclear magnetic resonance. The Journal of Chemical Physics 1996, 105 (3), 874-900. DOI: 10.1063/1.471968 (acccessed 10/8/2023).
(33) Gerothanassis, I. P.; Troganis, A.; Exarchou, V.; Barbarossou, K. NUCLEAR MAGNETIC RESONANCE (NMR) SPECTROSCOPY: BASIC PRINCIPLES AND PHENOMENA, AND THEIR APPLICATIONS TO CHEMISTRY, BIOLOGY AND MEDICINE. Chemistry Education Research and Practice 2002, 3 (2), 229-252, 10.1039/B2RP90018A. DOI: 10.1039/B2RP90018A.
(34) Passeri, D.; Dong, C.; Reggente, M.; Angeloni, L.; Barteri, M.; Scaramuzzo, F. A.; De Angelis, F.; Marinelli, F.; Antonelli, F.; Rinaldi, F.; et al. Magnetic force microscopy. Biomatter 2014, 4 (1), e29507. DOI: 10.4161/biom.29507.
(35) Vokoun, D.; Samal, S.; Stachiv, I. Magnetic Force Microscopy in Physics and Biomedical Applications. Magnetochemistry 2022, 8 (4), 42.
(36) Hartmann, U. MAGNETIC FORCE MICROSCOPY. Annual Review of Materials Science 1999, 29 (1), 53-87. DOI: 10.1146/annurev.matsci.29.1.53.
(37) Kazakova, O.; Puttock, R.; Barton, C.; Corte-León, H.; Jaafar, M.; Neu, V.; Asenjo, A. Frontiers of magnetic force microscopy. Journal of Applied Physics 2019, 125 (6). DOI: 10.1063/1.5050712 (acccessed 10/8/2023).
(38) Kong, L.; Chou, S. Y. Study of magnetic properties of magnetic force microscopy probes using micronscale current rings. Journal of Applied Physics 1997, 81 (8), 5026-5028. DOI: 10.1063/1.364499 (acccessed 10/8/2023).
(39) Sievers, S.; Braun, K.-F.; Eberbeck, D.; Gustafsson, S.; Olsson, E.; Schumacher, H. W.; Siegner, U. Quantitative Measurement of the Magnetic Moment of Individual Magnetic Nanoparticles by Magnetic Force Microscopy. Small 2012, 8 (17), 2675-2679. DOI: https://doi.org/10.1002/smll.201200420.
(40) Schreiber, S.; Savla, M.; Pelekhov, D. V.; Iscru, D. F.; Selcu, C.; Hammel, P. C.; Agarwal, G. Magnetic Force Microscopy of Superparamagnetic Nanoparticles. Small 2008, 4 (2), 270-278. DOI: https://doi.org/10.1002/smll.200700116.
(41) Makkinje, J.; Zimmerman, G. A Simple Apparatus for the Direct Measurement of Magnetic Forces and Magnetic Properties of Materials. 2014.
(42) Viswanadham, P. Inexpensive gouy balance for magnetic susceptibility determination. Journal of Chemical Education 1978, 55 (1), 54. DOI: 10.1021/ed055p54.
(43) Brubacher, L. J.; Stafford, F. E. Magnetic susceptibility: A physical chemistry laboratory experiment. Journal of Chemical Education 1962, 39 (11), 574. DOI: 10.1021/ed039p574.
(44) Saunderson, A. A permanent magnet Gouy balance. Physics Education 1968, 3 (5), 272. DOI: 10.1088/0031-9120/3/5/007.
(45) Davis, R. S. New method to measure magnetic susceptibility. Measurement Science and Technology 1993, 4 (2), 141. DOI: 10.1088/0957-0233/4/2/001.
(46) Reutzel, S.; Herlach, D. M. Measuring magnetic susceptibility of undercooled Co-based alloys with a Faraday balance. 2001, 3. DOI: https://doi.org/10.1002/1527-2648(200101)3:1/2<65::AID-ADEM65>3.3.CO;2-S
Journal Name: Advanced Engineering Materials; Journal Volume: 3; Journal Issue: 1-2; Other Information: 6 refs.; PBD: Jan 2001.
(47) Sandulyak, A.; Sandulyak, A.; Polismakova, M.; Ershova, V.; Sandulyak, D.; Kiselev, D. On the Issue of Choosing the Measuring Zones in a Faraday Balance When Studying Magnetic Susceptibility of Small Samples. Cham, 2018; Springer International Publishing: pp 77-83.
(48) Baskar, D.; Adler, S. B. High temperature Faraday balance for in situ measurement of magnetization in transition metal oxides. Review of Scientific Instruments 2007, 78 (2). DOI: 10.1063/1.2432476 (acccessed 10/8/2023).
(49) Sakakibara, T.; Mitamura, H.; Takashi Tayama, T. T.; Hiroshi Amitsuka, H. A. Faraday Force Magnetometer for High-Sensitivity Magnetization Measurements at Very Low Temperatures and High Fields. Japanese Journal of Applied Physics 1994, 33 (9R), 5067. DOI: 10.1143/JJAP.33.5067.

(50) Morris, B. L.; Wold, A. Faraday Balance for Measuring Magnetic Susceptibility. Review of Scientific Instruments 2003, 39 (12), 1937-1941. DOI: 10.1063/1.1683276 (acccessed 10/8/2023).
(51) Evans, D. F. A new type of magnetic balance. Journal of Physics E: Scientific Instruments 1974, 7 (4), 247. DOI: 10.1088/0022-3735/7/4/007.
(52) Kindra, D. R.; Evans, W. J. Magnetic Susceptibility of Uranium Complexes. Chemical Reviews 2014, 114 (18), 8865-8882. DOI: 10.1021/cr500242w.
(53) Dutta, S.; Mitra, A.; De, R.; Sardar, A.; Ghosh, S.; Maiti, T. Determination of Magnetic Susceptibility by Quincke's Method; 2013. DOI: 10.13140/RG.2.2.22086.88642.
(54) Parekh, K.; Upadhyay, R. Temperature dependence of magnetisation of magnetic fluid using Quincke's method. Indian Journal of Pure and Applied Physics 1997, 35, 523.
(55) Hayes, H. C. The Magnetic Susceptibility of Water. Physical Review 1914, 3 (4), 295-305. DOI: 10.1103/PhysRev.3.295.
(56) Richard Graybill, G.; Wrathall, J. W.; Ihrig, J. L. Magnetic Titration by a Modified Quincke Method. Instrumentation Science & Technology 1971, 3 (1), 71-87. DOI: 10.1080/10739147108543301.
(57) Michio, K.; Michihiko, K.; Masao, K.; Masaji, K. The Magnetic Susceptibility of Iodine in Various Solvents. Bulletin of the Chemical Society of Japan 1956, 29 (3), 305-307. DOI: 10.1246/bcsj.29.305.
(58) Ryabchikov, D. I.; Evgenia, A. T. e. PROGRESS IN METHODS FOR THE SEPARATION OF RARE-EARTH ELEMENTS. Russian Chemical Reviews 1960, 29 (10), 589. DOI: 10.1070/RC1960v029n10ABEH001256.
(59) Kołczyk-Siedlecka, K.; Wojnicki, M.; Kutyla, D.; Kowalik, R.; Zabinski, P.; Cristofolini, A. Separation of Ho3+ in Static Magnetic Field. Archives of Metallurgy and Materials 2016, 61. DOI: 10.1515/amm-2016-0308.
(60) Jensen, J.; Mackintosh, A. Rare Earth Magnetism: Structures and Excitations; 1991.
(61) Parker, D.; Suturina, E. A.; Kuprov, I.; Chilton, N. F. How the Ligand Field in Lanthanide Coordination Complexes Determines Magnetic Susceptibility Anisotropy, Paramagnetic NMR Shift, and Relaxation Behavior. Accounts of Chemical Research 2020, 53 (8), 1520-1534. DOI: 10.1021/acs.accounts.0c00275.
(62) Lei, Z.; Fritzsche, B.; Eckert, K. Evaporation-Assisted Magnetic Separation of Rare-Earth Ions in Aqueous Solutions. The Journal of Physical Chemistry C 2017, 121 (44), 24576-24587. DOI: 10.1021/acs.jpcc.7b07344.
(63) Yang, X.; Tschulik, K.; Uhlemann, M.; Odenbach, S.; Eckert, K. Enrichment of Paramagnetic Ions from Homogeneous Solutions in Inhomogeneous Magnetic Fields. The Journal of Physical Chemistry Letters 2012, 3 (23), 3559-3564. DOI: 10.1021/jz301561q.
(64) Boelens, P.; Lei, Z.; Drobot, B.; Rudolph, M.; Li, Z.; Franzreb, M.; Eckert, K.; Lederer, F. High-Gradient Magnetic Separation of Compact Fluorescent Lamp Phosphors: Elucidation of the Removal Dynamics in a Rotary Permanent Magnet Separator. Minerals 2021, 11. DOI: 10.3390/min11101116.
(65) Kołczyk-Siedlecka, K.; Kutyla, D.; Wojnicki, M.; Cristofolini, A.; Kowalik, R.; Zabinski, P. SEparation of rare earth metals ions in a static magnetic field. 2016, 52, 541-547.
(66) Wojtaszek, K.; Kołczyk-Siedlecka, K.; Cebula, F.; Michałek, T.; Wojnicki, M. ANALYSIS OF THE KINETICS IONS Ho(III), Pr(III), Gd(III) TRANSPORT AT THE LIQUID-LIQUID INTERFACE IN THE PRESENCE OF A MAGNETIC FIELD GRADIENT. 2022, 515-521. DOI: 10.22364/mhd.58.4.16.
(67) Kolczyk-Siedlecka, K.; Wojnicki, M.; Yang, X.; Mutschke, G.; Zabinski, P. Experiments on the magnetic enrichment of rare-earth metal ions in aqueous solutions in a microflow device. Journal of Flow Chemistry 2019, 9 (3), 175-185. DOI: 10.1007/s41981-019-00039-8.
(68) Franczak, A.; Binnemans, K.; Fransaer, J. Magnetomigration of rare-earth ions in inhomogeneous magnetic fields. Phys. Chem. Chem. Phys. 2016, 18. DOI: 10.1039/C6CP02575G.
(69) Pulko, B.; Yang, X.; Lei, Z.; Odenbach, S.; Eckert, K. Magnetic separation of Dy(III) ions from homogeneous aqueous solutions. Applied Physics Letters 2014, 105 (23). DOI: 10.1063/1.4903794 (acccessed 10/8/2023).
(70) Rodrigues, I. R.; Lukina, L.; Dehaeck, S.; Colinet, P.; Binnemans, K.; Fransaer, J. Magnetomigration of Rare-Earth Ions Triggered by Concentration Gradients. J Phys Chem Lett 2017, 8 (21), 5301-5305. DOI: 10.1021/acs.jpclett.7b02226 From NLM.
(71) Carvalho, R. S.; Daniel-da-Silva, A. L.; Trindade, T. Uptake of Europium(III) from Water using Magnetite Nanoparticles. Particle & Particle Systems Characterization 2016, 33 (3), 150-157. DOI: https://doi.org/10.1002/ppsc.201500170.
(72) Kreitman, M. M.; Milford, F. J.; Kenan, R. P.; Daunt, J. G. Magnetic Susceptibility of ${\mathrm{Mn}}^{2+}$ in CdS and Effects of Antiferromagnetic Exchange. Physical Review 1966, 144 (2), 367-372. DOI: 10.1103/PhysRev.144.367.
(73) Springer, S.; Butler, A. Magnetic susceptibility of Mn(III) complexes of hydroxamate siderophores. Journal of Inorganic Biochemistry 2015, 148. DOI: 10.1016/j.jinorgbio.2015.04.015.
(74) Benzie, R. J.; Cooke, A. H. The Magnetic Susceptibility of Copper Sulphate. Proceedings of the Physical Society. Section A 1951, 64 (2), 124. DOI: 10.1088/0370-1298/64/2/303.
(75) Kishita, M.; Muto, Y.; Kubo, M. Magnetic susceptibility of Tri-Coordinated copper(II) complexes. Australian Journal of Chemistry 1957, 10 (4), 386-391. DOI: https://doi.org/10.1071/CH9570386.
(76) Russell, C. D.; Cooper, G. R.; Vosburgh, W. C. Complex Ions. V. The Magnetic Moments of Some Complex Ions of Nickel and Copper1. Journal of the American Chemical Society 1943, 65 (7), 1301-1306. DOI: 10.1021/ja01247a014.
(77) Musher, J. I. On the Magnetic Susceptibility of Aromatic Hydrocarbons and ``Ring Currents". The Journal of Chemical Physics 2004, 43 (11), 4081-4083. DOI: 10.1063/1.1696645 (acccessed 8/23/2023).
(78) Popoli, A.; Pierotti, G.; Ragazzi, F.; Sandrolini, L.; Cristofolini, A. FLARE: A Framework for the Finite Element Simulation of Electromagnetic Interference on Buried Metallic Pipelines. Applied Sciences 2023, 13 (10), 6268.
(79) Popoli, A.; Ragazzi, F.; Pierotti, G.; Cristofolini, A. Inductive interference from HVAC power lines on metallic pipelines using FLARE - Finite eLement Analysis foR Electromagnetics. In 2023 IEEE International Conference on Environment and Electrical Engineering and 2023 IEEE Industrial and Commercial Power Systems Europe (EEEIC / I&CPS Europe), 6-9 June 2023, 2023; pp 1-6. DOI: 10.1109/EEEIC/ICPSEurope57605.2023.10194759.
(80) Gutiérrez-Mejía, F.; Ruiz-Suárez, J. C. AC magnetic susceptibility at medium frequencies suggests a paramagnetic behavior of pure water. Journal of Magnetism and Magnetic Materials 2012, 324 (6), 1129-1132. DOI: https://doi.org/10.1016/j.jmmm.2011.10.035.
(81) Pawlak, L.; Duczmal, M.; Pokrzywnicki, S. Interpretation of the ζ-Holmium Sesquiselenide Magnetic Susceptibility. In Crystalline Electric Field Effects in f-Electron Magnetism, Guertin, R. P., Suski, W., Zołnierek, Z. Eds.; Springer US, 1982; pp 473-478.
(82) Williams, E. H. Note on the Magnetic Properties of Rare Earth Oxides. Physical Review 1926, 27 (4), 484-486. DOI: 10.1103/PhysRev.27.484.
(83) Kuvandikov, O. K.; Shakarov, K. O.; Salakhitdiinova, M. K. Magnetic susceptibility of holmium compounds with iron group elements at high temperatures. Izvestiya Vysshikh Uchebnykh Zavedenij, Fizika 1997, 40 (6), 105-107.
(84) Moosavi, F.; Gholizadeh, M. Magnetic effects on the solvent properties investigated by molecular dynamics simulation. Journal of Magnetism and Magnetic Materials 2014, 354, 239-247. DOI: https://doi.org/10.1016/j.jmmm.2013.11.012.